Observational Study

Medicine®

OPEN

Altered directional connectivity between emotion network and motor network in Parkinson's disease with depression

Peipeng Liang, PhD[a,b,c], Gopikrishna Deshpande, PhD[d,e,f], Sinan Zhao, PhD[d], Jiangtao Liu, PhD[a], Xiaoping Hu, PhD[g,*], Kuncheng Li, PhD[a,b,c,*]

Abstract

Depression is common in patients with Parkinson's disease (PD), which can make all the other symptoms of PD much worse. It is thus urgent to differentiate depressed PD (DPD) patients from non-depressed PD (NDPD).

The purpose of the present study was to characterize alterations in directional brain connectivity unique to Parkinson's disease with depression, using resting state functional magnetic resonance imaging (rs-fMRI).

Sixteen DPD patients, 20 NDPD patients, 17 patients with major depressive disorder (MDD) and 21 healthy control subjects (normal controls [NC]) underwent structural MRI and rs-fMRI scanning. Voxel-based morphometry and directional brain connectivity during resting-state were analyzed. Analysis of variance (ANOVA) and 2-sample *t* tests were used to compare each pair of groups, using sex, age, education level, structural atrophy, and/or HAMD, unified PD rating scale (UPDRS) as covariates.

In contrast to NC, DPD showed significant gray matter (GM) volume abnormalities in some mid-line limbic regions including dorsomedial prefrontal cortex and precuneus, and sub-cortical regions including caudate and cerebellum. Relative to NC and MDD, both DPD and NDPD showed significantly increased directional connectivity from bilateral anterior insula and posterior orbitofrontal cortices to left inferior temporal cortex. As compared with NC, MDD and NDPD, alterations of directional connectivity in DPD were specifically observed in the pathway from bilateral anterior insula and posterior orbitofrontal cortices to right basal ganglia.

Resting state directional connectivity alterations were observed between emotion network and motor network in DPD patients after controlling for age, sex, structural atrophy. Given that these alterations are unique to DPD, it may provide a potential differential biomarker for distinguishing DPD from NC, NDPD, and MDD.

Abbreviations: ACC = anterior cingulate cortex, BDI = beck depression inventory, BOLD = blood oxygen level-dependent, CSF = cerebrospinal fluid, DAN = dorsal attention network, DASS = depression anxiety stress scales, DLPFC = dorsolateral prefrontal cortex, DMN = default mode network, DPARSF = data processing assistant for resting-state fMRI, DPD = depressed Parkinson's disease, EN = emotion network, EPI = echo-planar imaging, FA = flip angle, FOV = field of view, FWHM = full width at half maximum, GDS = Geriatric depression scale, GM = gray matter, H&Y = Hoehn and Yahr, HDRS = Hamilton rating scale for depression, IPL = inferior parietal lobule, LFF = low-frequency fluctuations, MADRS = Montgomery-Åsberg depression rating scale, MDD = major depressive disorder, MMSE = mini-mental state examination, MN = motor network, MPRAGE = magnetization-prepared rapid gradient echo, mVAR = multivariate autoregressive, NC = normal controls, NDPD = non-depressed Parkinson's disease, OFC = orbitofrontal cortex, PCC = posterior cingulate cortex, PD = Parkinson's disease, PHG = parahippocampal gyrus, QIDS = quick inventory of depressive symptomatology, rs-fMRI = resting state functional magnetic resonance imaging, TE = echo time, TI = inversion time, TR = repetition time, UPDRS = unified PD rating scale, WM = white matter.

Editor: Bernhard Schaller.

PL and GD havecontributed equally to this manuscript.

This work was supported by the Natural Science Foundation of China (61473196), Beijing Nova Program (Z12111000250000, Z131107000413120) and the Open Research Fund of the State Key Laboratory of Cognitive Neuroscience and Learning (CNLZD1302).

The funders had no role in study design, data collection and analysis, decision to publish, or preparation of the manuscript.

The authors have no conflicts of interest to disclose.

Supplemental Digital Content is available for this article.

[a] *Department of Radiology, Xuanwu Hospital, Capital Medical University, Beijing,* [b] *Beijing Key Lab of MRI and Brain Informatics, Beijing,* [c] *Key Laboratory for Neurodegenerative Diseases, Ministry of Education, PR China,* [d] *Auburn University MRI Research Center, Department of Electrical and Computer Engineering, Auburn University, Auburn, Alabama,* [e] *Department of Psychology, Auburn University, Auburn, Alabama,* [f] *Alabama Advanced Imaging Consortium, Auburn University and University of Alabama Birmingham, Alabama,* [g] *Wallace H Coulter Department of Biomedical Engineering, Georgia Institute of Technology and Emory University, Atlanta, Georgia.*

[*] *Correspondence: Xiaoping Hu, Wallace H. Coulter Department of Biomedical Engineering, Georgia Institute of Technology and Emory University, 101 Woodruff Circle, Suite 2001, Atlanta, GA 30322-4600 (e-mail: xhu@bme.gatech.edu); Kuncheng Li, Xuanwu Hospital, Capital Medical University, 45 Chang Chun Street, Xi Cheng District, Beijing 100053, China (e-mail: lkc1955@gmail.com).*

Medicine (2016) 95:30(e4222)

Received: 10 September 2015 / Received in final form: 31 May 2016 / Accepted: 20 June 2016

http://dx.doi.org/10.1097/MD.0000000000004222

Keywords: Effective connectivity, Major depressive disorder (MDD), Parkinson's disease with depression (DPD), Resting state functional MRI

1. Introduction

Depression is a common problem in patients with Parkinson's disease (PD),[1] and up to 50% of people with PD experience a major bout of depressive symptoms.[2,3] Depression can make all the other symptoms of PD much worse, including motor symptom deterioration, rapid disease progression, and cognitive attenuation,[4–6] and has been one of the major contributors to poor quality of life and disability in PD patients.[7] In addition, depression in individuals with PD has some unusual characteristics as compared with depression in individuals without PD, that is, major depressive disorder (MDD). As opposed to MDD, distinctive characteristics of depression in PD include more intense worrying, brooding, loss of interest, pessimism, hopelessness, suicidal tendencies, social withdrawal, self-depreciation, ideas of reference, and anxiety. Therefore, it is very imperative and urgent to characterize the underlying neural mechanisms of depressed PD (DPD) patients using neuroimaging methods.

Resting state functional MRI (rs-fMRI) has been widely used in the studies of neurological and psychiatric diseases, including MDD and PD, due to its practical advantages that patients are only required to "rest" without additional cognitive tasks or demands. Recently, some rs-fMRI studies have been performed to examine the underlying neural substrates and the imaging biomarkers of DPD patients. All these previous studies focus on regional deficits[8] and/or functional connectivity abnormalities of a specific network.[9–11] These results revealed impairments of many brain regions in the motor network, default mode network, and emotion network as well as many functional pathways among these networks in DPD patients, as compared with non-depressed PD (NDPD) and normal controls (NC).

However, previous studies mainly focused on the comparison of DPD and NDPD,[8–11] without explicitly comparing DPD and MDD. Given that DPD is the comorbidity of PD and depression, any potentially specific biomarker should differentiate DPD from both NDPD and MDD. Additionally, although previous functional connectivity findings have demonstrated that DPD is possibly a disconnection syndrome, whether the causal directional connectivity profile of DPD is significantly altered is still unclear. This is an important question because synchronization (as measured by non-directional functional connectivity) and causality (as measured by directional effective connectivity) are distinct modes of communication in the human brain. Another important concern is that brain atrophy may cause a partial volume effect in functional imaging results,[12] especially in neurodegenerative diseases.[13–17] However, in previous DPD-related studies, anatomical and functional brain deficits were examined in different samples and the potential impact of atrophy on the functional results were not accounted.

Given the above considerations, we recruited 4 groups of subjects in this study, including DPD, NDPD, MDD, and NC, and simultaneously collected their structural MRI and rs-fMRI data. The main goal of the current study is to examine the causal connectivity differences in DPD as compared with NDPD, MDD, and NC after controlling for structural atrophy. We examined the causal connectivity patterns of DPD patients within and between 4 important brain networks, including the default mode network (DMN),[18,19] the dorsal attention network (DAN),[20] motor network (MN)[21], and emotion network (EN).[22] These functional brain networks have been widely confirmed by using resting state functional connectivity, as measured using low-frequency fluctuations (LFF) (<0.1 Hz) of the blood oxygen level-dependent (BOLD) signal. DMN and DAN are 2 basic functional networks since the former is engaged in internally directed cognition and the latter in externally directed cognition.[20,23] In particular, DPD patients have significant motor (in contrast to NC and MDD) and emotion related impairment (in contrast to NC and NDPD), it is thus of direct interest to examine the connectivity within DMN, DAN, EN, and MN, and the interactions between them.

We tested the hypothesis that there would be causal disconnections within and between the 4 networks in DPD patients as compared with NC. Particularly, given that DPD is likely to have elements of both NDPD and MDD, we hypothesized that there would be abnormal causal connectivity between MN and EN specifically for DPD patients when compared with NDPD, MDD, and NC, which could potentially form a specific and unique neural signature of DPD.

2. Materials and methods

2.1. Subjects

This study was approved by the Medical Research Ethics Committee of Xuanwu Hospital, Beijing, China. Seventy-four right-handed subjects (16 DPD, 20 NDPD, 17 MDD, and 21 NC) participated in this study and written informed consent was obtained from each participant. All PD patients were recruited from the outpatient clinic at Xuanwu Hospital from September 2014 to September 2015. Detailed demographic data of the participants are shown in Table 1. All patients were off medication for 12 hours when they came in for imaging and neuropsychological testing.

Thirty-six patients with idiopathic PD were recruited from the movement disorders outpatient clinics of Xuanwu Hospital. All PD patients were diagnosed based on the UK PD Society Brain Bank Clinical Diagnostic Criteria.[24] The Unified PD Rating Scale (UPDRS) part III[25,26] was used to assess motor disability, and Hoehn and Yahr (H&Y) stage[27] was used to evaluate disease severity. All PD patients had normal cognitive function as measured by a score on the Mini-Mental State Examination (MMSE) of 27 or more. Sixteen of these PD patients were diagnosed with major depression disorder according to the Diagnostic and Statistical Manual of Mental Disorders, 5th edition (DSM-V) criteria (American Psychiatric Association), and the remaining 20 patients had PD alone. The 25-item Hamilton Rating Scale for Depression (HDRS), Beck Depression Inventory (BDI), and Geriatric Depression Scale (GDS) were recorded to evaluate the severity of depression. Patients were excluded if they had: moderate to severe head tremor; a history of head injury, stroke, or other neurologic disease; abnormal MMSE scores; and any disorder that interfered with the assessment of the manifestation of PD.

Patients with major depression were recruited from Anding Hospital from September 2014 to September 2015. All MDD patients were diagnosed according to the Structured Clinical Interview of the DSM-V (SCID). Depression severity was assessed

Table 1

Demographics and clinical findings.

	DPD (N = 16)	NDPD (N = 20)	MDD (N = 17)	NC (N = 21)	*P*
Sex, women/men	10/6	10/10	11/6	8/13	0.33*
Age, year	63.5 ± 9.87	61.0 ± 10.46	46.47 ± 8.66	56.43 ± 6.45	<0.05†
Time since diagnosis, year	6.31 ± 5.51	5.75 ± 2.61	6.0 ± 3.24	/	0.34†
HRSD	15.88 ± 3.85	4.0 ± 2.37	21.24 ± 4.75	/	<0.01†
UPDRS	39.87 ± 19.25	36.96 ± 14.32	/	/	0.68‡
MMSE	29.51 ± 0.53	29.24 ± 2.21	/	/	0.91‡
HY	2.13 ± 1.89	1.52 ± 0.96	/	/	0.66‡
BDI	19.57 ± 7.66	8.30 ± 5.37	/	/	<0.01‡
GDS	21.21 ± 4.25	10.46 ± 6.43	/	/	<0.01‡
LED (mg/d)	565.99 ± 323.91	544.44 ± 376.71	/	/	0.964‡
MADRS	/	/	30.24 ± 8.69	/	
QIDS	/	/	21.15 ± 7.20	/	
DASS-depression	/	/	11.46 ± 5.26	/	
DASS-anxiety	/	/	7.62 ± 4.86	/	
DASS-stress	/	/	7.15 ± 4.80	/	

Values are means ± SD.

BDI = Beck depression inventory, DASS = Depression anxiety stress scales, DPD = depressed Parkinson's disease, GDS = Geriatric depression scale, HRSD = Hamilton rating scale for depression, HY = Hoehn-Yahr, MADRS = Montgomery–Åsberg depression rating scale, MDD = major depressive disorder, MMSE = Mini Mental state examination, NC = normal controls, NDPD = non-depressed Parkinson's disease, QIDS = quick inventory of depressive symptomatology, UPDRS = Unified Parkinson's Disease Rating Scale.

* The *P* value was obtained using a chi-squared test.

† The *P* value was obtained using one-way ANOVA.

‡ The *P* value was obtained by a 2-sample 2-tailed *t* test.

using HDRS, and further assessed using Montgomery-Åsberg Depression Rating Scale (MADRS), Quick Inventory of Depressive Symptomatology (QIDS), and the depression scale of Depression Anxiety Stress Scales (DASS). Anxiety severity was assessed using the anxiety scale of DASS and stress severity was evaluated using the stress scale of DASS. Exclusion criteria for MDD patients included: other psychiatric disorders such as schizophrenia, schizoaffective disorder, bipolar disorders, or severe personality disorders or mental retardation, assessed with SCID; a history of organic brain disorders, neurological disorders, cardiovascular diseases or other serious physical illness provided by personal history or laboratory analysis.

In addition, 21 right-handed healthy controls were recruited from the local community through advertisements. Healthy controls were assessed by a neurologist for their neuropsychiatric condition. Control subjects were excluded if they had: a history or present diagnosis of any Diagnostic and Statistical Manual of Mental Diseases disorders; any neurologic illness, as assessed by clinical evaluations and medical records; or organic brain defects on T1 or T2 images.

2.2. MRI data acquisition

MRI data were acquired on a SIEMENS 3 Tesla Trio scanner (Siemens, Erlangen, Germany). Foam padding and headphones were used to limit head motion and reduce scanner noise. The subjects were instructed to hold still, keep their eyes closed, and think nothing in particular. Functional images were collected axially using an echo-planar imaging (EPI) sequence (repetition time [TR]/echo time [TE]/flip angle [FA]/field of view [FOV] = 2000 ms/40 ms/90°/24 cm, resolution = 64 × 64 matrix, slices = 28, thickness = 4 mm, gap = 1 mm, bandwidth = 2232 Hz/pixel). The scan lasted for 478 seconds. 3D T1-weighted magnetization-prepared rapid gradient echo (MPRAGE) sagittal images were collected by using the following parameters: TR/TE/inversion time (TI)/FA = 1900 ms/2.2 ms/900 ms/9°, resolution = 256 × 256 matrix, slices = 176, thickness = 1.0 mm.

2.3. FMRI data preprocessing

Unless otherwise stated, all analyses were conducted using Data Processing Assistant for Resting-State fMRI (DPARSF)[28] and statistical parametric mapping software package (SPM8, http://www.fil.ion.ucl.ac.uk/spm). The first 10 volumes of the functional images were discarded to allow the signal to reach equilibrium and participants' adaptation to the scanning noise. The remaining 229 fMRI volumes were first corrected for within-scan acquisition time differences between slices and spatially realigned to the first volume to correct for inter-scan head motion. No participant had head motion of more than 1.5 mm displacement in any of the x, y, or z directions and larger than 1.5° of rotation throughout the course of the scan. The individual structural images were co-registered to the mean functional images after motion correction using a linear transformation. The transformed structural images were then segmented into gray matter (GM), white matter (WM), and cerebrospinal fluid (CSF) by using a unified segmentation algorithm.[29] The motion corrected functional volumes were spatially normalized to the Montreal Neurological Institute (MNI) space and re-sampled to 3 mm isotropic voxels using the normalization parameters estimated during unified segmentation. Subsequently, the functional images were spatially smoothed with a Gaussian kernel of $6 \times 6 \times 6\,mm^3$ full width at half maximum (FWHM) to decrease spatial noise. Following this, temporal filtering ($0.01\,Hz < f < 0.08\,Hz$) was applied to the time series of each voxel to reduce the effect of low-frequency drifts and high-frequency noise. To further reduce the effects of confounding factors, we also used a linear regression process to remove the effects of head motion and other possible sources of artifacts by regressing out: 6 motion parameters, WM and CSF time series.

2.4. Region of interest definition

Forty-nine Region of interests (ROIs) from 4 resting state brain networks, including the default mode network (DMN), dorsal attention network (DAN), motor network (MN), and emotion

network (EN) were selected. Table 2 lists the Talairach coordinates of the ROIs of all 4 networks. Coordinates of the 49 ROIs were defined according to peer-reviewed published literature. The ROIs of DMN were defined according to Grecius et al,[19] which included posterior cingulate cortex (PCC), left/right posterior inferior parietal lobule (L/R pIPL), orbitofrontal cortex/ventral anterior cingulate cortex (OFC/vACC), dorsomedial prefrontal cortex Brodmann area 8 (dMPFC BA8), dorsomedial prefrontal cortex Brodmann area 9 (dMPFC BA9), left dorsolateral prefrontal cortex (L DLPFC), left parahippocampal gyrus (L PHG), and left inferolateral temporal cortex (L ITC). The ROIs of DAN were chosen based on coordinates reported by Vincent et al.[30] Accordingly, DAN was composed of left/right middle temporal area (L/R MT), left/right frontal eye fields (L/R FEF), and left/right superior parietal lobule (L/R SPL). The ROIs of MN were determined based on several publications,[31–36] and included bilateral sensorimotor cortices, supplementary motor area (SMA), left ventral premotor cortex (vPMC), bilateral inferior parietal cortex (L/R IPC), bilateral basal ganglia (L/R BG), bilateral anterior cerebellum. The ROIs of EN were defined according to Kober et al,[22] and involved visual area 8/bilateral superior cerebellum (V8/sCB [Bi]), bilateral middle temporal complex (MT+ [Bi]), right visual area 4 (V4 [R]), right lateral occipital cortex/temporal lobe (latOCC/Temp [R]), PCC, primary visual cortex (V1), dorsal medial prefrontal cortex (dmPFC), pregenual anterior cingulate cortex (pgACC), rostral dorsal anterior cingulate cortex (rdACC), ventral anterior insula/frontal operculum/right temporal pole, bilateral posterior orbitofrontal cortex (vaIns/frOP/TP [R] pOFC [Bi]), bilateral anterior insula, posterior orbitofrontal cortex (aINS pOFC [Bi]), bilateral ventral anterior insula/temporal cortex/orbitofrontal cortex (vaIns/TC/OFC JCN [Bi]), bilateral middle insula, right dorsal putamen (midIns [Bi] dPut [R]), left ventral Striatum, middle insula, hippocampus (VSTR midIns HCMP [L]), left Basolateral Amygdala (BL Amy [L]), hypothalamus (Hy), periaqueductal gray/thalamus (PAG/Thal), bilateral amygdala, ventral striatum (Cau/Put), ventral globus pallidus, thalamus (Amy vStr vGP Thal [Bi]), right frontal operculum (frOP [R]), right inferior frontal gyrus (IFG [R]), left pre-supplementary motor area, inferior frontal gyrus (preSMA, IFG [L]).

Table 2

The Talairach coordinates of the selected ROIs in DMN, DAN, MN and EN. The abbreviations are as described in the main text.

Networks	Peak Talairach coordinates		
	x	y	z
Default mode network			
PCC	−2	−51	27
L pIPL	−51	−65	27
R pIPL	53	−61	27
OFC/vACC	−2	55	−18
dMPFC BA 8	−16	49	38
dMPFC BA 9	18	54	32
L DLPFC	−44	20	41
R DLPFC	44	20	41
L PHG	−12	−35	0
R PHG	12	−35	0
L ITC	−58	−18	−14
R ITC	58	−18	−14
Dorsal attention network			
L MT	−43	−66	−4
R MT	45	−66	−4
L FEF	−25	−13	48
R FEF	23	14	48
L SPL	−27	−55	50
R SPL	20	−59	49
Motor network			
L sensorimotor cortices	−38	−23	47
R sensorimotor cortices	36	−19	51
SMA	−4	−5	48
L vPMC	−53	0	30
L IPC	−50	−24	20
R IPC	40	−39	42
L BG	−22	−8	4
R BG	22	−9	6
L anterior cerebellum	−22	−49	23
R anterior cerebellum	16	−49	−14
Emotion network			
V8/sCB (Bi)	−11	−61	−14
MT+ (Bi)	−28	−66	12
V4 (R)	44	−77	0
latOCC/Temp (R)	49	−54	1
PCC	1	−51	26
V1	−7	−86	4
dmPFC	−2	51	24
pgACC	1	38	0
rdACC	0	29	22
valns/frOP/TP (R) pOFC (Bi)	38	18	−10
alNS pOFC (Bi)	−40	22	−6
valns/TC/OFC JCN (Bi)	−7	11	−20
midIns (Bi) dPut (R)	21	0	2
VSTR midIns HCMP (L)	−36	0	−7
BL Amy (L)	−23	−4	−17
Hy	−7	−5	−11
PAG/Thal	−1	−22	3
Amy vStr vGP Thal (Bi)	11	−6	−8
frOP (R)	46	24	4
IFG (R)	49	20	16
preSMA, IFG (L)	−23	14	33

DAN = dorsal attention network, DMN = default mode network, EN = emotion network, MN = motor network.

Using a sub-function of the "GingerALE" software package (http://brainmap.org/ale/) called "icbm2tal," the coordinates in previous studies were transformed from MNI space to Talairach space. ROIs were 12 mm spheres centered at the corresponding coordinates and were masked by a template consisting of only those voxels that were inside the brain using WFU PickAtlas toolbox (www.ansir.wfubmc.edu). Consequently, the sizes of some of the ROIs differed slightly. It can be seen that the coordinates of the PCC region with the same name but appearing in both DMN and EN are a little different. Consistent with previous studies,[17,37] we considered them separately as part of distinct networks without merging them. It was hypothesized that if their functional roles are similar because of anatomical proximity, then the functional similarity will be reflected in the results of our analysis. Four ROIs had an overlap. They were R MT of DAN and V4 (R) of EN, and R BG of MN and midIns (Bi) dPut (R) of EN. Average time courses for the ROIs were generated for each ROI and subject. For the 4 ROIs that had an overlap, the average time courses were computed from the non-overlapping voxels in those regions. Subsequently, for every ROI, the time series corresponding to each subject was concatenated to obtain one time series per ROI.[37,38]

2.5. Regional GM atrophy

GM intensity maps were obtained by the unified segmentation algorithm[29] as described in the Data preprocessing section. After spatially smoothing with a Gaussian kernel of 10 mm FWHM, a

one-way analysis of variance (ANOVA) was performed on the smoothed GM intensity maps to examine the group differences of regional GM atrophy among 4 groups, using sex, age, and education level as covariates. The statistical threshold was set at $P<0.01$ and cluster size ≥119 voxels, which corresponded to a corrected $P<0.05$ (using the AlphaSim program). A 2-sample t test was also applied to examine the between-group differences. When comparing DPD and NC, sex, age, and education level were used as covariates; when comparing DPD and NDPD, sex, age, education level, and UPDRS were used as covariates; when comparing DPD and MDD, sex, age, education level, and Hamilton Rating Scale for Depression (HRSD) were used as covariates.

2.6. Directional connectivity analysis

Suppose $X(t)=(x_1(t),x_2(t)\ldots x_k(t))^T$ be the k selected ROI time series. In order to account for the zero-lag correlation effect, a modified multivariate autoregressive (mVAR) model used by Deshpande et al[39] for calculating Granger causality is as follows:

$$X(\mathrm{t})=\sum_{n=0}^{p}A(\mathrm{n})\,X(\mathrm{t}-\mathrm{n})+\mathrm{E}(\mathrm{t})$$

Where $A(n)$ are the coefficients of the model with order p and E (t) is the model error. The diagonal elements of the zero-lag term $A(0)$ were set to zero to model only the instantaneous cross-correlation between time series instead of the auto-correlation of each time series. On the other hand, the off-diagonal elements of $A(0)$ correspond to zero-lag correlation. Since instantaneous cross-correlation is modeled out in the zero-lag term $A(0)$, the causal relationship obtained from $A(1)\ \ldots\ A(p)$ are purged of correlation leakage effects,[37] thus termed as correlation-purged Granger causality (CPGC). Direct causal influence between the k selected ROI time series can be obtained from the model parameters as follows:

$$CPGC_{ij}=\sum_{n=1}^{p}(\mathrm{a}_{ij})^2(\mathrm{n})$$

Where a_{ij} are the elements of the matrix $\boldsymbol{A}$ and $CPGC_{ij}$ denotes the direct causal influence from ROI j to ROI i.

All the steps of effective connectivity analysis are identical to what is reported in Deshpande et al.[38] First, after standard preprocessing, the mean time series were extracted from 49 ROIs of the 4 networks for each subject, then entered into a fifth order mVAR model[40–42] to obtain the correlation-purged causal connectivity between them. The order of the mVAR model was determined using Bayesian Information Criterion (BIC). The model order of 5 was determined by estimating the lowest BIC corresponding to the best fit of the model and parameter parsimony.[43] Surrogate data were obtained from the ROI time series by randomizing their phase, but retaining the magnitude power spectrum, and input into the mVAR model. The above procedure was repeated 10,000 times to derive empirical null distributions for each path. A flow chart illustrating the connectivity analysis pipeline is shown in Fig. 1.

2.7. Statistical analysis

The CPGC values were entered into a 2-sample t test to identify the significant differences between DPD and the other 3 groups (i.e., NC, NDPD, and MDD), using sex, age, education level, and structural atrophy (measured by voxel-based morphometry) as covariates. Additionally, when comparing DPD and NDPD, UPDRS was also used as a covariate to control for the disease severity; when comparing DPD and MDD, HRSD was also used as a covariate to control for different depression levels. The causal paths (bi-directional or uni-directional) surviving a threshold of $P<0.01$ (false discovery rate (FDR) corrected) were considered to show significant group difference. The comparison of most interest in this study is the common paths of the 3 contrasts, that is, DPD versus NC, DPD versus NDPD, and DPD versus MDD.

3. Results

As shown in Table 1, there were significant differences among the 4 groups of participants for age ($P<0.05$) but not for sex. There was no significant difference among DPD, NDPD, and MDD in

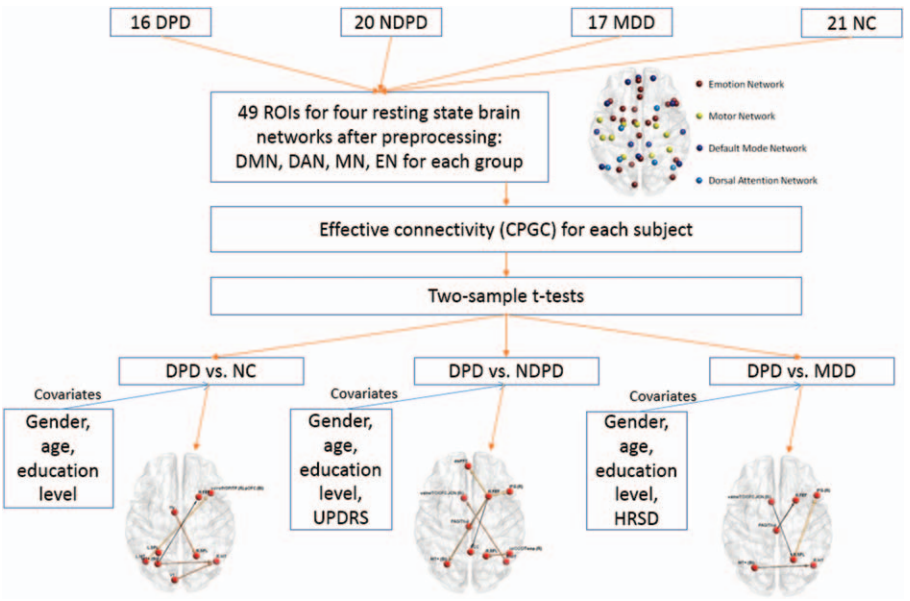

Figure 1. The flow chart illustrating the connectivity analysis pipeline.

disease duration, but HRSD was significantly different ($P < 0.01$). UPDRS, MMSE, HY, and levodopa equivalent dose were not significantly different between DPD and NDPD while BDI ($P < 0.01$) and GDS ($P < 0.01$) were significant. The head motion during the rs-fMRI scanning was not significantly different between the 4 groups ($P > 0.05$).

3.1. VBM results

The results of one-way ANOVA showed that the 4 groups had significantly different GM volume in the left superior medial frontal gyrus (BA 10), left medial frontal gyrus (BA 32), left superior temporal gyrus (BA 22), left precuneus (BA 7), right precentral gyrus (BA 6), right supramarginal gyrus (BA 40), bilateral thalamus, right caudate, and left cerebellum posterior lobe (Fig. 2A). The paired-wise comparisons showed that DPD exhibited significant GM intensity difference from the other 3 groups of participants (Table 3). As compared with controls, DPD showed significant GM atrophy in the right caudate, left superior medial frontal gyrus (BA 10) and left medial frontal gyrus (BA 32) (Fig. 2B). As compared with NDPD, DPD showed significant GM atrophy in the left precuneus (BA 40) and right cerebellum posterior lobe (Fig. 2C). In contrast to MDD, DPD showed significantly increased GM intensity in the precuneus (BA 40) (Fig. 2D).

3.2. Causal connectivity

As compared with NC, DPD showed significant differences in many causal paths, including both within-network (within MN, EN) and between-network (MN-DMN, MN-DAN, MN-EN, EN-DMN, EN-DAN) pathways. Similarly, we also observed the significant differences between DPD and NDPD, as well as between DPD and MDD. The detailed between-group results can be found in the supplementary materials (Figure S1–S39, http://links.lww.com/MD/B143).

Of most interest and relevance to our hypothesis, 2 causal paths were identified to be common in the comparisons of "DPD versus NDPD ", "DPD versus MDD" and "DPD versus NC". As shown in Fig. 3, the 2 paths were aINS.pOFC.(Bi) → L.ITC and aINS.pOFC.(Bi) → R.BG. The former was stronger in DPD as compared with both NC and MDD, but weaker as compared with NDPD. The latter was stronger in DPD as compared with all the other groups. We also investigated the sex effect among the 2 common paths. It was found that the path aINS.pOFC.(Bi) → R. BG was significantly greater in DPD women as compared with DPD men ($P = 0.03$), while this sex difference was not evident in NDPD, MDD, and NC groups.

In particular, as the age difference between groups is a little higher, the dependence may still exist even after using age as a covariate of no interest. Thus, we further run an analysis to see if the mean squared error of the model is correlated with age. If not, it means that the effect of age has been completely regressed out. It was found that the model error is not correlated with age ($P > 0.1$). Therefore, the model has effectively regressed out the effect of age.

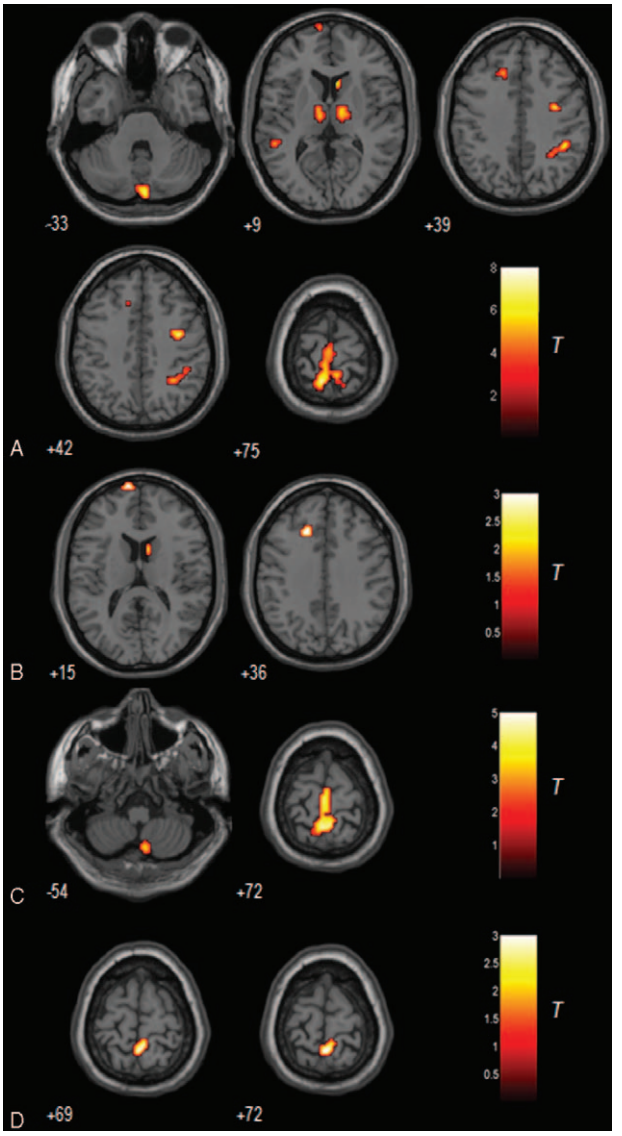

Figure 2. A. The grey matter differences among 4 groups using analysis of covariance (ANCOVA). B. The grey matter difference between NC and DPD (hot = NC > DPD). C. The grey matter difference between NDPD and DPD (hot = NDPD > DPD). D. The grey matter difference between MDD and DPD (hot = DPD > MDD). The threshold was set to a cluster size of 22 voxels with uncorrected $P < 0.01$, which corresponds to a corrected $P < 0.01$ determined by the Monte Carlo simulations with the program AlphaSim in AFNI, with mask file: BrainMask_05_61*73*61.img (70831 voxels, under REST_DIR mask directory). DPD = depressed Parkinson's disease, MDD = major depressive disorder, NC = normal controls, NDPD = non-depressed Parkinson's disease.

4. Discussion

The novelty of the present study lies in the fact that we used directional connectivity analysis to investigate the underlying biological markers of DPD. Results showed that there was significant within- and between-networks causal disconnection in DPD in contrast to NDPD, MDD, and NC (Figure S1–37, http://links.lww.com/MD/B143) after controlling for sex, age, and structural atrophy. In particular, the strength of aINS.pOFC(Bi) → L ITC was significantly increased in both DPD and NDPD, as compared with MDD and NC, and the pathway of aINS.pOFC (Bi) → R BG was significantly elevated in DPD in contrast to the other 3 groups. Moreover, women DPD patients showed greater connectivity of aINS. pOFC(Bi) → R BG than man DPD patients.

Some ROIs in this study have overlaps (although the average time courses were computed from the non-overlapped regions), which could potentially confound the final results. Further analysis was then performed by reducing the radius to 3 mm to make the ROIs non-overlapping and it did not show any change

Table 3

GM differences between DPD patients and the other 3 groups.

Brain regions	MNI coordinate			BA	Cluster size	*T*-score
	x	*y*	*z*			
NC > DPD						
Rt. Caudate	9	15	6		22	2.94
Lt. superior medial frontal gyrus	−9	69	15	10	21	3.23
Lt. medial frontal gyrus	−18	30	33	32	27	−3.53
DPD > NDPD						
Lt. precuneus	−3	−48	75	40	190	4.94
Rt. cerebellum posterior lobe	6	−69	−54		27	3.42
DPD > MDD						
Precuneus	0	−48	72	40	22	3.06

DPD = depressed Parkinson's disease, GM = gray matter, MDD = major depressive disorder, MNI = Montreal Neurological Institute, BA = Brodmann Area, NC = normal controls, NDPD = non-depressed Parkinson's disease.

in the patterns of the results except for statistical power. Additionally, an alternative ROI definition method is to perform an independent component analysis (ICA) to identify study-specific resting state network regions. Accordingly, we performed ICA on all subjects (i.e. by not differentiating the groups), found resting state networks (RSNs) for the entire sample, back projected them onto individual subjects, obtained time series from each RSN in individual subjects and then re-ran the directional connectivity analysis. It was found that all the 4 RSNs could be identified. DMN regions included PCC, MPFC, and bilateral IPL; DAN regions contained bilateral FEF and SPL; MN regions consisted of the bilateral sensorimotor area, SMA, and bilateral cerebellum; and EN regions mainly comprised bilateral amygdala, dmPFC, and PCC. However, some functional regions previously reported in larger cohorts and which were included among our 49 ROIs, were not identified by ICA. For example, hippocampus and bilateral ITC were not found in DMN, BG was not detected in MN, and insula was not found in EN. Additionally, PCC in DMN still had a slight overlap with PCC in EN. Given these limitations, we report the findings based on the 49 functional ROIs (from previous publications) in order to fully explore the connectivity difference between different groups of subjects.

By using causal connectivity analysis, this study revealed the impairment of MN and EN in DPD patients, consistent with previous studies.[8,10,11] Furthermore, the current study has extended the previous studies by identifying the aberrant interactions among MN, EN, DMN, and DAN in DPD. These results provide new evidence for the notation that DPD can be characterized as a functional disconnection syndrome. The unique connectivity signatures of DPD as compared with NDPD and MDD further suggest that DPD is not a simple superposition of NDPD and MDD.

Previous studies have reported distributed regions with significant GM reductions in DPD patients, including the orbitofrontal cortex (OFC), insula, thalamus, medial temporal gyrus, etc.[3,44–47] However, previous VBM studies did not show convergent results. For example, OFC reduction was detected in 2 studies,[44,45] but not in the other studies.[3,46,47] A reduction in this region was not observed in our study either. Many factors may contribute to these inconsistencies, including diagnostic criteria, sex, age, disease duration, sample size, and so on. In the present study, structural alterations, as well as causal connectivity changes were investigated in the same sample. With GM structural atrophy, age and sex modeled as effects of no interest in this study, the abnormal causal connectivity identified in DPD

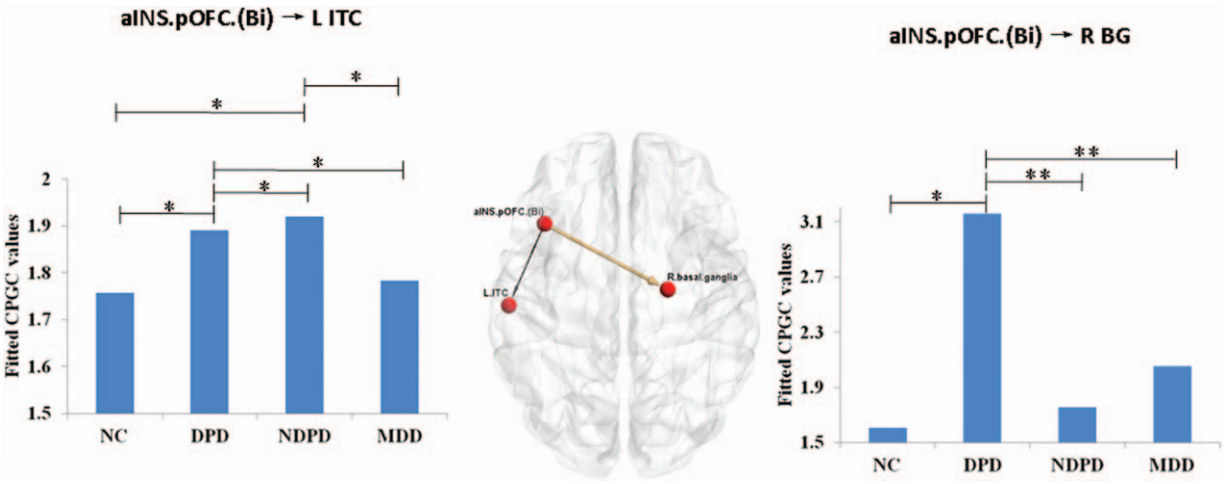

Figure 3. Two directed pathways which were common in the 3 comparisons of "DPD versus NDPD ", "DPD versus MDD" and "DPD versus NC ". The strength of causal connectivity was plotted together with the statistical power. * represents $P < 0.05$; ** represents $P < 0.01$. DPD = depressed Parkinson's disease, MDD = major depressive disorder, NC = normal controls, NDPD = non-depressed Parkinson's disease.

in the current study are independent of structural alterations, age, and sex.

Compared to MDD and NC, both NDPD and DPD showed enhanced connectivity of aINS.pOFC.(Bi) → L.ITC pathway; however, DPD had stronger connectivity on this pathway than NDPD. This finding supports the point of view that depression may result from neurodegenerative changes occurring in PD.[48,49] Insula and OFC play important roles in EN. The insula has structural and functional connections with the cingulate, amygdala, and orbitofrontal cortex, and contributes to the conscious experience of emotion in general.[50] OFC is thought to represent emotion and reward in decision-making.[51] As a key part of DMN, ITC is essential for episodic/declarative memory.[52] Thus, the increased connectivity exerted from insula/OFC to ITC may indicate that negative emotions potentially induced by the disease are encoded/processed into the memory system, which may exacerbate the disease in PD.[53]

In the current study, the abnormally enhanced aINS.pOFC.(Bi) → R.BG connectivity was observed specifically in DPD patients, in contrast to NDPD, MDD, and NC. BG, especially the putamen, is known to play an important role in MN for preparing and aiding in the movement of the limbs. Signals are transmitted through BG to the motor thalamus, brain stem, and motor neocortex, helping the body learn movement as well as aiding in movements. Thus, the current finding indicated that EN exerted an influence on motor functions specifically in DPD patients. One possible explanation for the increased causal connectivity between EN and MN is that it may reflect the anomalous interactions between the 2 networks and may further increase disability. An alternative explanation may relate it to functional compensation for the impaired motor functions. Although some previous authors have associated hyper-connectivity with functional compensation,[54,55] many others have considered increases in connectivity as a reflection of functional disruption[56] and altered neuronal communication.[57] It is therefore considered that "functional disconnection" implies both functional hypo-connectivity and hyper-connectivity. The current data did not allow us to make a choice between the 2 competing interpretations. Additionally, the significantly stronger connectivity of aINS.pOFC.(Bi) → R.BG in women DPD patients than men may be a potential neural substrate underlying sex difference in this disease.[58]

Finally, we would like to note certain limitations of the current study. First, being a preliminary study, our sample size was modest, enough to make statistical inferences but not enough to make strong conclusions about the generalizability of the results. Second, sex and age of the MDD and NC groups were not well matched with the DPD and NDPD groups. To control for the effect of age and sex, we included them as covariates in the statistical analysis. Third, some neurological measures were not tested for all groups of subjects. For example, MDD patients were not tested with UPDRS. Given that pharmacological treatments for MDD could potentially cause the appearance of Parkinsonian motor signs, this should be taken into consideration in the future. Finally, results obtained from Granger causality analysis of fMRI data should be interpreted with some caveats in mind. Specifically, Abler et al[59] demonstrated using a simple auditory-motor paradigm that Granger causality can correctly estimate expected causal influences from the auditory cortex to the motor cortex even with fMRI data acquired with long TRs (2440 ms in their study). As they argue, significant Granger causality obtained from slowly sampled fMRI data is likely to correctly reflect corresponding neural causality, though a lack of significant Granger causality obtained from such fMRI data does not imply a corresponding lack of directional influence at the neural level. This limitation needs to be kept in mind while interpreting results presented here.

In conclusion, this study has extended our knowledge beyond previous findings by demonstrating unique directional brain connectivity signatures underlying DPD, which are distinct from NDPD, MDD, and NC. The current findings provide novel insights into the pathophysiological mechanism of DPD patients and highlight the potential of using directional brain connectivity as potential imaging biomarkers.

References

[1] Santamaria J, Tolosa E, Valles A. Parkinson's disease with depression: a possible subgroup of idiopathic parkinsonism. Neurology 1986;36:1130–3.

[2] Ehrt U, Br∅nnick K, Leentjens AFG, et al. Depressive symptom profile in Parkinson's disease: a comparison with depression in elderly patients without Parkinson's disease. Int J Geriatr Psychiatry 2006;21:252–8.

[3] Cardoso EF, Maia FM, Fregni F, et al. Depression in Parkinson's disease: convergence from voxel-based morphometry and functional magnetic resonance imaging in the limbic thalamus. Neuroimage 2009;47:467–72.

[4] Starkstein SE, Preziosi TJ, Forrester AW, et al. Specificity of affective and autonomic symptoms of depression in Parkinson's disease. J Neurol Neurosurg Psychiatry 1990;53:869–73.

[5] Marder K, Tang MX, Cote L, et al. The frequency and associated risk factors for dementia in patients with Parkinson's disease. Arch Neurol 1995;52:695–701.

[6] Kuhn W, Heye N, Muller T, et al. The motor performance test series in Parkinson's disease is influenced by depression. J Neural Transm 1996;103:349–54.

[7] Storch A, Ebersbach G, Fuchs G, et al. Depression in Parkinson's disease. Part 1: epidemiology, signs and symptoms, pathophysiology and diagnosis. Fortschr Neurol Psychiatr 2008;76:715–24.

[8] Wen X, Wu X, Liu J, et al. Abnormal baseline brain activity in non-depressed Parkinson's disease and depressed Parkinson's disease: a resting-state functional magnetic resonance imaging study. PLoS One 2013;8:e63691.

[9] Sheng K, Fang W, Su M, et al. Altered spontaneous brain activity in patients with Parkinson's disease accompanied by depressive symptoms, as revealed by regional homogeneity and functional connectivity in the prefrontal-limbic system. PLoS One 2014;9:e84705.

[10] Luo C, Chen Q, Song W, et al. Resting-state fMRI study on drug-naive patients with Parkinson's disease and with depression. J Neurol Neurosurg Psychiatry 2014;85:675–83.

[11] Hu X, Song X, Yuan Y, et al. Abnormal functional connectivity of the amygdala is associated with depression in Parkinson's disease. Mov Disord 2015;30:238–44.

[12] Bokde AL, Pietrini P, Ibanez V, et al. The effect of brain atrophy on cerebral hypometabolism in the visual variant of Alzheimer disease. Arch Neurol 2001;58:480–6.

[13] Oakes TR, Fox AS, Johnstone T, et al. Integrating VBM into the general linear model with voxelwise anatomical covariates. Neuroimage 2007;34:500–8.

[14] He Y, Wang L, Zang Y, et al. Regional coherence changes in the early stages of Alzheimer's disease: a combined structural and resting-state functional MRI study. Neuroimage 2007;35:488–500.

[15] Liang P, Wang Z, Yang Y, et al. Functional disconnection and compensation in mild cognitive impairment: evidence from DLPFC connectivity using resting-state fMRI. PLoS ONE 2011;6:e22153.

[16] Liang P, Wang Z, Yang Y, et al. Three subsystems of the inferior parietal cortex are differently affected in mild cognitive impairment. J Alzheimers Dis 2012;30:475–87.

[17] Liang P, Li Z, Deshpande G, et al. Altered causal connectivity of resting state brain networks in amnesic MCI. PLoS One 2014;9:e88476.

[18] Raichle ME, Macleod AM, Snyder AZ, et al. A default mode of brain function. Proc Natl Acad Sci USA 2001;98:676–82.

[19] Grecius M, Krasnow B, Reiss A, et al. Functional connectivity in the resting brain: a network analysis of the default mode hypothesis. Proc Natl Acad Sci USA 2003;100:253–8.

[20] Fox MD, Snyder AZ, Vincent JL, et al. The human brain is intrinsically organized into dynamic, anticorrelated functional networks. Proc Natl Acad Sci USA 2005;102:9673–8.

[21] Biswal B, Yetkin FZ, Haughton VM, et al. Functional connectivity in the motor cortex of resting human brain using echo-planar MRI. Magn Reson Med 1995;34:537–41.
[22] Kober H, Barrett LF, Joseph J, et al. Functional grouping and cortical-subcortical interactions in emotion: a meta-analysis of neuroimaging studies. Neuroimage 2008;42:998–1031.
[23] Fransson P. Spontaneous low-frequency BOLD signal fluctuations: an fMRI investigation of the resting-state default mode of brain function hypothesis. Hum Brain Mapp 2005;26:15–29.
[24] Hughes AJ, Daniel SE, Kilford L, et al. Accuracy of clinical diagnosis of idiopathic Parkinson's disease: a clinico-pathological study of 100 cases. J Neurol Neurosurg Psychiatry 1992;55:181–4.
[25] Goetz CG, Tilley BC, Shaftman SR, et al. Movement Disorder Society UPDRS Revision Task ForceMovement disorder society-sponsored revision of the Unified Parkinson's Disease Rating Scale (MDS-UPDRS): scale presentation and clinimetric testing results. Mov Disord 2008;23:2129–70.
[26] Hacker CD, Perlmutter JS, Criswell SR, et al. Resting state functional connectivity of the striatum in Parkinson's disease. Brain 2012;135(Pt 12):3699–711.
[27] Hoehn MM, Yahr MD. Parkinsonism: onset, progression and mortality. Neurology 1967;17:427–42.
[28] Yan CG, Zang YF. DPARSF: a MATLAB toolbox for "Pipeline" data analysis of resting-state fMRI. Front Syst Neurosci 2010;4:13.
[29] Ashburner J, Friston KJ. Unified segmentation. Neuroimage 2005;26:839–51.
[30] Vincent JL, Kahn I, Snyder AZ, et al. Evidence for a frontoparietal control system revealed by intrinsic functional connectivity. J Neurophysiol 2008;100:3328–42.
[31] Mitz AR, Godschalk M, Wise SP. Learning-dependent neuronal activity in the premotor cortex: activity during the acquisition of conditional motor associations. J Neurosci 1991;11:1855–72.
[32] Shadmehr R, Holcomb HH. Neural correlates of motor memory consolidation. Science 1997;277:821–5.
[33] Padoa-Schioppa C, Li CS, Bizzi E. Neuronal activity in the supplementary motor area of monkeys adapting to a new dynamic environment. J Neurophysiol 2004;91:449–73.
[34] Doyon J, Bellec P, Amsel R, et al. Contributions of the basal ganglia and functionally related brain structures to motor learning. Behav Brain Res 2009;199:61–75.
[35] Pasalar S1, Roitman AV, Durfee WK, et al. Force field effects on cerebellar Purkinje cell discharge with implications for internal models. Nat Neurosci 2006;9:1404–11.
[36] Steele CJ, Penhune VB. Specific increases within global decreases: a functional magnetic resonance imaging investigation of five days of motor sequence learning. J Neurosci 2010;30:8332–41.
[37] Deshpande G, LaConte S, James G, et al. Multivariate Granger causality analysis of brain networks. Hum Brain Mapp 2009;30:1361–73.
[38] Deshpande G, Santhanam P, Hu X. Instantaneous and causal connectivity in resting state brain networks derived from functional MRI data. Neuroimage 2011;54:1043–52.
[39] Deshpande G, Li Z, Santhanam P, et al. Recursive cluster elimination based support vector machine for disease state prediction using resting state functional and effective brain connectivity. PLoS One 2010;5:e14277.
[40] Deshpande G, Sathian K, Hu X. Effect of hemodynamic variability on Granger causality analysis of fMRI. Neuroimage 2010;52:884–96.
[41] Deshpande G, Sathian K, Hu X. Assessing and compensating for zero-lag correlation effects in time-lagged Granger causality analysis of fMRI. IEEE Trans Biomed Eng 2010;57:1446–56.
[42] Deshpande G, Hu X, Lacey S, et al. Object familiarity modulates effective connectivity during haptic shape perception. Neuroimage 2010;49:1991–2000.
[43] Schwartz G. Estimating the dimension of a model. Ann Stat 1978;5:461–4.
[44] Feldmann A, Illes Z, Kosztolanyi P, et al. Morphometric changes of gray matter in Parkinson's disease with depression: a voxel-based morphometry study. Mov Disord 2008;23:42–6.
[45] Kostić VS, Filippi M. Neuroanatomical correlates of depression and apathy in Parkinson's disease: magnetic resonance imaging studies. J Neurol Sci 2011;310:61–3.
[46] Surdhar I, Gee M, Bouchard T, et al. Intact limbic-prefrontal connections and reduced amygdala volumes in Parkinson's disease with mild depressive symptoms. Parkinsonism Relat Disord 2012;18:809–13.
[47] van Mierlo TJ, Chung C, Foncke EM, et al. Depressive symptoms in Parkinson's disease are related to decreased hippocampus and amygdala volume. Mov Disord 2015;30:245–52.
[48] Burn DJ. Depression in Parkinson's disease. Eur J Neurol 2002;9:44–54.
[49] McDonald WM, Richard IH, Delong MR. Prevalence, etiology, and treatment of depression in Parkinson's disease. Biol Psychiatry 2003;54:363–75.
[50] Suzuki A. Emotional functions of the insula. Brain Nerve 2012;64:1103–12.
[51] Rolls ET, Grabenhorst F. The orbitofrontal cortex and beyond: From affect to decision-making. Prog Neurobiol 2008;86:216–44.
[52] Buckner R, Andrews-Hanna J, Schacter D. The brain's default network: anatomy, function and relevance to disease. Ann NY Acad Sci 2008;1124:1–38.
[53] Nuti A, Ceravolo R, Piccinni A, et al. Psychiatric comorbidity in a population of Parkinson's disease patients. Eur J Neurol 2004;11:315–20.
[54] Hillary FG, Roman CA, Venkatesan U, et al. Hyperconnectivity is a fundamental response to neurological disruption. Neuropsychology 2015;29:59–75.
[55] Wang L, Zang Y, He Y, et al. Changes in hippocampal connectivity in the early stages of Alzheimer's disease: evidence from resting state fMRI. Neuroimage 2006;31:496–504.
[56] Esposito F, Pignataro G, Di Renzo G, et al. Alcohol increases spontaneous BOLD signal fluctuations in the visual network. Neuroimage 2010;53:534–43.
[57] Licata SC, Nickerson LD, Lowen SB, et al. The hypnotic zolpidem increases the synchrony of BOLD signal fluctuations in widespread brain networks during a resting paradigm. Neuroimage 2013;70:211–22.
[58] Scott B, Borgman A, Engler H, et al. Gender differences in Parkinson's disease symptom profile. Acta Neurol Scand 2000;102:37–43.
[59] Abler B, Roebroeck A, Goebel R, et al. Investigating directed influences between activated brain areas in a motor-response task using fMRI. Magn Reson Imaging 2006;24:181–5.